International Journal of Fracture, Vol. 11, No. 2, April 1975
Noordhoff International Publishing – Leyden
Printed in The Netherlands

An assumed displacement hybrid finite element model for linear fracture mechanics*

SATYA N. ATLURI

School of Engineering Science and Mechanics, Georgia Institute of Technology, Atlanta, Georgia 30332, *U.S.A.*

ALBERT S. KOBAYASHI and MICHIHIKO NAKAGAKI

Department of Mechanical Engineering, University of Washington, Seattle, Washington 98195, *U.S.A.*

(Received October 25, 1973; in revised form August 9, 1974)

ABSTRACT

This paper deals with a procedure to calculate the elastic stress intensity factors for arbitrary-shaped cracks in plane stress and plane strain problems. An assumed displacement hybrid finite element model is employed wherein the unknowns in the final algebraic system of equations are the nodal displacements and the elastic stress intensity factors. Special elements, which contain proper singular displacement and stress fields, are used in a fixed region near the crack tip; and the interelement displacement compatibility is satisfied through the use of a Lagrangean multiplier technique. Numerical examples presented include: central as well as edge cracks in tension plates and a quarter-circular crack in a tension plate. Excellent correlations were obtained with available solutions in all the cases. A discussion on the convergence of the present solution is also included.

1. Introduction

Among the several approximate methods currently available for elastic stress analysis of cracks, the finite element method has the advantage of easy adaptation to problems with complex geometries, anisotropic materials, non-homogeneous material properties, or complex cases of combined mechanical and thermal loading. For two-dimensional problems, the method of finite element analysis has been used extensively to determine Mode I stress intensity factors [2–6] as well as some mixed modes I and II stress intensity factors. Stress intensity factor was obtained by either curve-fitting the proper singular stress or displacement with the approximate stress distribution or crack opening displacement (COD) obtained by the finite element method. Thus very small element breakdown was required in the vicinity of the crack tip in order to accurately calculate the near field stresses and displacements. More recently strain energy release rate [4, 5] has been used to estimate stress intensity factors with relatively coarse finite element grids. This approach provided better accuracy than the COD approach, but the two modes of crack tip deformation could not be separated conveniently.

It should be mentioned that Refs. [2–6] do not contain any studies of convergence of such a method when applied to problems of cracks involving singularities. Tong and Pian [7], in a recent paper, have shown that, for problems with singularities, the convergence rates of the finite element method are dominated by the singular nature of solution near the crack tip, unless these singularities are properly incorporated in the assumed functions, the regular so-called high-accuracy elements (with higher-order polynomials as interpolates) will not be able to improve the rate of convergence.

The special element used by Byskov [8] and Tracy [9] did not satisfy the inter-element boundary compatibility criteria. Thus, convergence of such a solution cannot be guaranteed, as has been proven by Tong and Pian [10]. Levy, *et al.* [11], used a special element which was

* This work was supported by the U.S. Air Force Office of Scientific Research, Grant AFOSR-73-2478.

derived mainly for elastic-perfectly-plastic material, containing a r^{-1} type strain singularity, but only gave a very qualitative discussion of the accuracy of the stress intensity factor.

Pian, Tong, and Luk [12] used a special crack-tip finite element with the correct singularities, of the $r^{-\frac{1}{2}}$ type for elastic analysis, included in the assumed stresses. This special element was derived by a procedure similar to the hybrid stress model originated by Pian [13].

The results of [12] showed that the stress intensity factors can be calculated accurately by using a much smaller number of degrees of freedom than by using only conventional elements. Tong, Pian and Lasry [14] have recently improved upon the analysis of [12] by combining the hybrid element concept with those of the complex variable techniques developed by Bowie in his modified boundary collocation method for crack problems [15, 16, 17]. The hybrid stress model, however, has not been used thus far for elastic-plastic analysis in the presence of plastic yielding surrounding the crack tip.

For fracture problems involving large scale yielding in the vicinity of the crack tip, the elastic-plastic state surrounding the crack tip must be known. Unfortunately, other than the known solutions [18, 19] in Mode III crack tip deformation, there exist no solutions involving single or compound Modes I and II crack tip deformation in the presence of plastic yielding. The work of Rice and Rosegren [20] and Hutchinson [21, 22] predicts a r^{-1} type of singularity for strains, and possibly no singularity in stresses for a perfectly plastic solid. Thus a finite element hybrid model which contains r^{-1} singularity in strains, but non-singular stresses, would thus be a possible choice for the elastic-plastic analysis of the cracked structure. With this motivation, research was initiated into the application of the assumed displacement hybrid finite element model [23, 24] to study the elastic-plastic stress states around cracks.

In the present paper, we discuss the application of such a hybrid displacement model to two-dimensional plane problems. The discussion will be limited to the linear elastic case, but arbitrary anisotropic material properties are considered.

2. Formulation of hybrid displacement model

In the following only cartesian tensors are used. The variational principle which governs the assumed displacement hybrid model [23, 24] is a modified principle of minimum potential energy for which the functional to be varied is,

$$'\pi_{\mathrm{HD}} = \Sigma_m \{ \int_{V_m} (\tfrac{1}{2} E_{ijkl} \varepsilon_{ij} \varepsilon_{kl} - \bar{F}_i u_i) \mathrm{d}V + \int_{\partial V_m} T_{Li}(v_i - u_i) \mathrm{d}S - \int_{S_{\sigma_m}} \bar{T}_i v_i \mathrm{d}S \} \tag{1}$$

where V_m is the volume of an element, ∂V_m is the boundary of V_m, S_{σ_m} is the portion of ∂V_m where the surface traction $\bar{T}_i$ is given, and E_{ijkl} is the given elastic-compliance tensor. In the above $\varepsilon_{ij} \equiv \frac{1}{2}(u_{i,j} + u_{j,i})$, where u_i are differentiable displacement functions within V_m, but need not be continuous across the boundary of V_m. The function v_i is the inter-element boundary displacement which is continuous on ∂V_m and subject to the condition that $v_i = \bar{u}_i$ on $S_{u_m} \cdot S_{u_m}$ is the portion of ∂V_m over which disp acement $\bar{u}_i$ is assigned. $\bar{F}_i$ is the body force and T_{Li} is the boundary traction on ∂V_m. Thus, in a solution of an elasticity problem, the quantities u_i, v_i, and T_{Li} are treated as unknown variables in the above functional. It can be seen that when the functional in Eqn. (1) is varied with respect to u_i, v_i and T_{Li}, one obtains,

$$\begin{aligned} \delta\pi = \Sigma_m \{ & - \int_{V_m} [(E_{ijkl}\varepsilon_{kl})_{,j} + \bar{F}_i] \delta u_i \mathrm{d}V + \int_{\partial V_m} T_{Li} \delta v_i \mathrm{d}S \\ & + \int_{\partial V_m} (E_{ijkl}\varepsilon_{kl} v_j - T_{Li}) \delta u_i \mathrm{d}S + \int_{\partial V_m} (v_i - u_i) \delta T_{Li} \mathrm{d}S - \int_{S_{\sigma_m}} \bar{T}_i \delta v_i \mathrm{d}S \} \end{aligned} \tag{2}$$

The vanishing of $\delta\pi$ for arbitrary δu_i in V_m, for arbitrary δT_{Li} on ∂V_m, and for admissible δv_i on ∂V_m such that $\delta V_i = 0$ on S_{u_m}, can be shown to give the Euler equations,

$$(E_{ijkl}\varepsilon_{kl})_{,j} + \bar{F}_i = 0 \text{ in } V_m \tag{3}$$

$$u_i = v_i \text{ on } \partial V_m \tag{4}$$

$$E_{ijkl}\varepsilon_{kl}v_j - T_{Li} = 0 \text{ on } \partial V_m \tag{5}$$

$$T_{Li} = \overline{T}_i \text{ on } S_{\sigma_m} \tag{6}$$

where

$$\varepsilon_{ij} = \tfrac{1}{2}(u_{i,j} + u_{j,i}) . \tag{7}$$

Thus, of all the admissible functions u_i defined in V_m, and T_{Li} and v_i defined on ∂V_m, those functions that render the functional π_{HD} of Eqn. (1) stationary, satisfy the Eqns. (3–6). Equation (3) states the fact that the displacement functions u_i in V_m generate stresses $\{\frac{1}{2}E_{ijkl}(u_{i,j}+u_{j,i})\}$ that satisfy the local equilibrium equation in V_m. Equation (4) states the fact that the values of u_i at ∂V_m coincide with the interelement boundary displacement v_i which is treated as an independent unknown. Equation (5) states the fact that the boundary tractions T_{Li}, which are treated as independent unknowns in the present problem, coincide with the tractions $\frac{1}{2}E_{ijkl}(u_{k,l}+u_{l,k})v_j$ generated at ∂V_m by the functions u_i.

Since v_i is the same for two adjacent elements on their common boundary, Eqn. (4) thus enforces *a posteriori* the condition that u_i of one element is equal to u_i of its neighboring element at their common boundary. Thus it can be seen that the hybrid finite element model enables one to choose element displacement functions that are completely arbitrary and need not satisfy the inter-element compatibility condition. This inter-element compatibility is enforced *a posteriori* by introducing the inter-element boundary displacement v_i as an independent variable and enforcing the constraint condition $v_i = u_i$ on ∂V_m. This constraint condition is introduced in the variational formulation through the boundary integral $\int_{\partial V_m} T_{Li}(v_i - u_i)\mathrm{d}S$ appearing in Eqn. (1). For this reason, the boundary tractions T_{Li} on ∂V_m, which are treated as independent variables in the present problem, can also be viewed mathematically as Lagrangean multipliers.

In the application of this model to crack problems, one can visualize the domain of the problem to be divided into two regions: (a) a small region near the crack tip where the singular, near field solution is predominant and (b) a region away from the crack tip where the effect of the singularity is not felt.

We shall first consider the development of the properties of a finite element in the vicinity of a crack tip (Fig. 1). In the present formulation, for which the nature of displacement behavior near the crack tip is known, it is a simple matter to include the correct behavior of displacements in the assumed approximate functions for u_i in the elements in the vicinity of the crack tip. Thus, within the finite element near the crack tip, we can assume

$$\begin{aligned}\{u_i\}_S &= [U_R]\{\beta\} + [U_S]\begin{Bmatrix} K_I \\ K_{II} \end{Bmatrix} \\ &\equiv [U_R]\{\beta\} + [U_S]\{K_S\}\end{aligned} \tag{8}$$

where U_R are simple polynomials, β are unknown independent parameters, K_I and K_{II} are stress intensity factors for Mode I and Mode II crack behavior, and U_S are known displacement functions for plane problems which yield the correct singular behavior for stresses and strains in linear elastic analysis. The functions U_S can easily be obtained from known analytical near field solutions for plane crack problems, and are shown in Appendix A.

Second, we assume an independent element boundary displacement. This assumed inter-element boundary displacement is such that it can be uniquely interpolated by displacements at the nodes along the boundary. Since these nodes are common for elements that share the common boundary, inter-element boundary displacement compatibility is thus insured. For the elements adjacent to the crack tip (see Fig. 1), a $r^{\frac{1}{2}}$ type displacement behavior is built in to the boundary displacements along lines AB, AC, and AD. After considerable numerical experimentation it was also concluded that for boundary lines, such as BE, DE, etc., only a quadratic polynomial displacement assumption is adequate. It should be

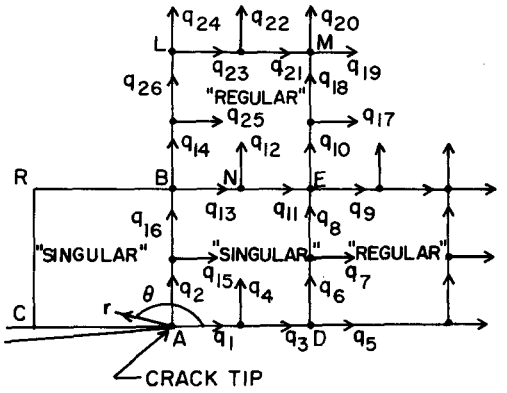

Figure 1a. Arrangement of "singular" and "regular" elements.

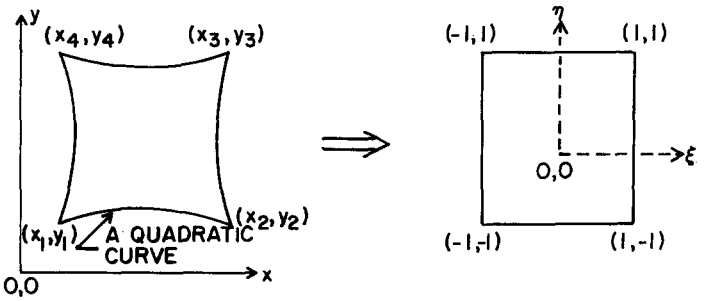

Figure 1b. Isoparametric transformation.

noted at this point that all elements other than those surrounding the crack tip such as ABRC, ABED, are so-called regular elements with only ordinary polynomial distributions of displacements and stresses. Moreover, at the boundary line such as BE, between a singular element (such as ABED) and a regular element (such as BLME) the displacement distributions are quadratic polynomials and are uniquely interpolated from their respective values at the three nodes *B*, *N*, and *E*. Thus, the inter-element displacement compatibility along line BE is satisfied. Thus, for *singular element* such as ABED, the boundary displacements, v_i are interpolated as

$$\underset{8\times 1}{\{v_i\}_S} = \underset{8\times 16}{[L_S]} \underset{16\times 1}{\{\ q\ \}} \tag{9}$$

where $[L_S]$ is the matrix of appropriate boundary interpolation functions as discussed above, and q's are the appropriate element nodal displacements. The matrix $[L_S]$ is given in Appendix A.

Thirdly, we assume element boundary tractions (which can also be identified as Lagrangean multipliers in the present formulation) for a singular element such as ABED. In this regard, we first note the relevant Euler equation of the variational formulation, *viz.*, Eqn. (5), which states that the boundary tractions generated by the assumed interior displacements u_i (*viz.*, $\frac{1}{2}E_{ijkl}(u_{k,l}+u_{l,k})v_j$) must match the independently assumed boundary tractions T_{Li}. Since the assumed displacements u_i for the singular element (such as ABED) contain a $r^{\frac{1}{2}}$ type behavior, they will generate singular boundary tractions of the $r^{-\frac{1}{2}}$ type along the boundary. Thus, for numerical accuracy in the present formulation, the assumed tractions T_{Li} for a

singular element such as ABED must also contain a $r^{-\frac{1}{2}}$ type behavior, to be compatible with those generated by u_i. Based on the above considerations, the boundary tractions T_{Li} for a singular element such as ABED are assumed independently, as

$$\underset{8\times 1}{\{T_{Li}\}_S} = [R_S]\{\alpha\} \tag{10}$$

where the functions in matrix R_S are given in Appendix A. At this point it is worth noting that, since the boundary tractions in the present formulation are being assumed independently, for better numerical accuracy, one could enforce *a priori* any stress free conditions on the crack surface. This can be done by simply assuming zero tractions on the crack surface.

Equations (8, 9, 10) and Eqns. (A.1, A.2, A.3) in Appendix A give: (a) the assumed interior displacements u_i; (b) assumed boundary displacements v_i; and (c) assumed boundary tractions T_{Li}, necessary for the formulation of the hybrid stress model, for the so-called singular element in the vicinity of a crack tip in a plane problem. Similar assumptions for u_i, v_i and T_{Li} for elements away from the crack tip are far easier to generate because, one can, for these elements assume simple polynomials. For regular elements, we thus note, the relevant assumptions can be written as

$$\{u_i\} = [U_R]\{\beta\} \tag{11}$$

$$\{v_i\} = [L_R]\{q\} \tag{12}$$

$$\{T_{Li}\} = [R_R]\{\alpha\}\,. \tag{13}$$

Substituting of Eqns. (8, 9, 10) and (11, 12, 13) into Eqn. (1) and noting that out of a total of N elements in the structure only a certain number of elements in the vicinity of the crack tip, say elements $m=1$ to $m=p$, are the so-called singular elements, we obtain the following expression

$$\begin{aligned}\pi_{HD} = {} & \Sigma_{1\leq m\leq p}\tfrac{1}{2}[\beta][H_1]\{\beta\} + [\beta][H_2]\{K_s\} \\ & + \tfrac{1}{2}[K_s][H_3]\{K_s\} - [\beta]\{F_1\} - [K_s]\{F_2\} \\ & + [q][G]\{\alpha\} - [\beta][P_1]\{\alpha\} - [K_s][P_2]\{\alpha\} - [q]\{F_3\} \\ & + \Sigma_{p+1\leq m\leq N}\tfrac{1}{2}[\beta][H_1^*]\{\beta\} - [\beta]\{F_1^*\} + [q][G^*]\{\alpha\} - [\beta][P_1^*]\{\alpha\} - [q]\{F_3^*\}\,.\end{aligned} \tag{14}$$

Before proceeding to define the several matrices in Eqn. (14), we first note that the relevant strains that are derived from the assumed displacements as in Eqn. (8) and (11) can be defined as,

$$\{\varepsilon\} = \{\tfrac{1}{2}(u_{i,j}+u_{j,i})\} = [W_R]\{\beta\} + [W_s]\{K_s\} \tag{15}$$

for singular elements ($m=1, \ldots, p$) and

$$\{\varepsilon\} = [W_R]\{\beta\} \tag{16}$$

for regular elements ($m=p+1, \ldots, N$). Making use of Eqns. (15) and (16), we now define the matrices in Eqn. (14) thus:

$$[H_1] = \int_{V_m}[W_R]^T\,[E][W_R]\,dV \qquad (m=1, \ldots, p) \tag{17a}$$

$$[H_2] = \int_{V_m}[W_R]^T[E][W_s]\,dV \qquad (m=1, \ldots, p) \tag{17b}$$

$$[H_3] = \int_{V_m}[W_s]^T[E][W_s]\,dV \qquad (m=1, \ldots, p) \tag{17c}$$

$$\{F_1\} = \int_{V_m}[U_R]^T\{\bar{F}_i\}\,dV \qquad (m=1,\ldots,p) \tag{17d}$$
$$\{F_2\} = \int_{V_m}[U_s]^T\{\bar{F}_i\}\,dV \qquad (m=1,\ldots,p) \tag{17e}$$
$$[G] = \int_{\partial V_m}[L_s]^T[R_s]\,dS \qquad (m=1,\ldots,p) \tag{17f}$$
$$[P_1] = \int_{\partial V_m}[U_R]^T[R_s]\,dS \qquad (m=1,\ldots,p) \tag{17g}$$
$$[P_2] = \int_{\partial V_m}[U_s]^T[R_s]\,dS \qquad (m=1,\ldots,p) \tag{17h}$$
$$\{F_3\} = \int_{S_\sigma}[L_s]^T\{\bar{T}_i\}\,dS \qquad (m=1,\ldots,p) \tag{17i}$$

and

$$[H_1^*] = \int_{V_m}[W_R]^T[E][W_R]\,dV \qquad (m=p+1,\ldots,N) \tag{17j}$$
$$\{F_1^*\} = \int_{V_m}[U_R]^T\{\bar{F}_i\}\,dV \qquad (m=p+1,\ldots,N) \tag{17k}$$
$$[G^*] = \int_{\partial V_m}[L_R]^T[R_R]\,dS \qquad (m=p+1,\ldots,N) \tag{17l}$$
$$[P_1^*] = \int_{\partial V_m}[U_R]^T[R_R]\,dS \qquad (m=p+1,\ldots,N) \tag{17m}$$
$$\{F_3^*\} = \int_{\partial V_m}[L_R]^T\{\bar{T}_i\}\,dS \qquad (m=p+1,\ldots,N) \tag{17n}$$

In the above, $[E]$ is the arbitrary elastic constant matrix. In Eqn. (14), the parameters β and α are independent for each of the elements, $m=1,\ldots,N$, whereas the parameters q (nodal displacements) and K_s (the stress intensity factors) are common to the entire system of elements. Taking variations of π_{HD} in Eqn. (14) with respect to the independent β's and α's for each element, we obtain the following equations:

(i) for elements $m=1,\ldots,p$:

$$[H_1]\{\beta\}+[H_2]\{K_s\}-\{F_1\}-[P_1]\{\alpha\}=0 \tag{18a}$$
$$[G]^T\{q\}-[P_1]^T\{\beta\}-[P_2]^T\{K_s\}=0 \tag{18b}$$

(ii) for elements $m=p+1,\ldots,N$:

$$[H_1^*]\{\beta\}-\{F_1^*\}-[P_1^*]\{\alpha\}=0 \tag{19a}$$
$$[G^*]^T\{q\}-[P_1^*]^T\{\beta\}=0\,. \tag{19b}$$

From Eqns. (18a, b) and (19a, b) one can express the parameters α and β of each element in terms of the quantities q of the respective element, and K_I and K_{II} and thus retain only the q's and K_I, K_{II} as the independent parameters in the functional in Eqn. (14). Thus,

(i) for elements $m=1,\ldots,P$:

$$\{\beta\} = [P_1^{-1}]^T([G]^T\{q\}-[P_2^T]\{K_s\}) \tag{20a}$$
$$\{\alpha\} = [P_1^{-1}]([H_1][P_1]^{-T}[G]^T\{q\}-[H_1][P_1]^{-T}[P_2^T]\{K_s\}+[H_2]\{K_s\}-\{F_1\}) \tag{20b}$$

(ii) for elements $m=p+1,\ldots,N$:

$$\{\beta\} = [P_1^*]^{-T}[G^*]^T\{q\} \tag{21a}$$
$$\{\alpha\} = [P_1^*]^{-1}[H_1^*][P_1^*]^{-T}[G^*]^T\{q\}-[P_1^*]^{-1}\{F_1^*\}\,. \tag{21b}$$

In Eqns. (20a, b) and (21a, b) the matrices $[P_1]$ and $[P_1^*]$ are assumed to be square and invertible. This can be easily achieved by properly choosing as many β's (Eqns. 8, 11) as α's (Eqns. 10 and 13), thus making matrices P_1 and P_1^* square and invertible. Substituting for β's and α's for each element ($m=1,\ldots,N$) from Eqns. (20a, b) and (21a, b) in Eqn. (14), one can express the functional π_{HD} in terms of nodal displacements q and stress intensity factors K_I and K_{II} only as follows:

$$\pi_{HD} = \Sigma_{1\leq m\leq p}\tfrac{1}{2}[q][K_{m1}]\{q\}+\tfrac{1}{2}[K_s][K_{m3}]\{K_s\}$$
$$+[K_s][K_{m2}]\{q_s\}-[q]\{R_1\}-[K_s]\{R_2\}+\Sigma_{p+1\leq m\leq N}\tfrac{1}{2}[q][K_m]\{q\}-[q]\{R\} \tag{22}$$

where

$$[K_{m1}] = [G][P_1^{-1}][H_1][P_1]^T[G]^T \text{ for } m=1,\ldots,p$$

$$[K_{m2}] = [H_2]^T[P_1]^{-T}[G]^T-[P_2][P_1^{-1}][H_1][P_1]^{-T}[G]^T \quad m=1,\ldots,p$$

$$[K_{m3}] = [P_2][P_1]^{-1}[H_1][P_1]^{-T}[P_2]^T+[H_3]-2[P_2][P_1]^{-1}[H_2] \quad m=1,\ldots,p$$

$$\{R_1\} = [G][P_1]^{-1}\{F_1\}+\{F_3\}$$

$$\{R_2\} = \{F_2\}-[P_2][P_1]^{-1}\{F_1\}$$

and

$$[K_m] = [G^*][P_1^*]^{-1}[H_1^*][P_1^*]^{-T}[G^*]^T \qquad m=p+1,\ldots,N$$
$$\{R\} = [G^*][P_1^*]^{-1}\{F_1\}+\{F_2^*\} \qquad m=p+1,\ldots,N \tag{23}$$

By expressing the element nodal displacements q in terms of independent generalized global displacements q^* (the transformation from q to q^* might also involve a coordinate transformation) and by realising that $[K_s]$ is common for elements ($m=1, p$) we can write

$$\pi_{HD} = \tfrac{1}{2}[q^*][\boldsymbol{K}_1]\{q_1^*\}+[K_s][\boldsymbol{K}_2]\{q^*\}$$
$$+\tfrac{1}{2}[K_s][\boldsymbol{K}_3]\{K_s\}-[q^*]\{Q_1\}-[K_s]\{Q_2\} \tag{24}$$

where $\boldsymbol{K}_1$, $\boldsymbol{K}_2$, $\boldsymbol{K}_3$, Q_1 and Q_2 are the *global* matrices which are obtained by assembling the corresponding element matrices. The stationary condition of π_{HD} in Eqn. (24) with respect to q^* and K_s then yields,

$$[\boldsymbol{K}_1]\{q^*\}+[\boldsymbol{K}_2]^T\{K_s\} = \{Q_1\} \tag{25a}$$

and

$$[\boldsymbol{K}_2]\{q^*\}+[\boldsymbol{K}_3]\{K_s\} = \{Q_2\}\,. \tag{25b}$$

The solution of Eqns. (25a, b) yield the nodal displacements q^* of the entire structure, and the stress-intensity factors K_I and K_{II} for the mixed-mode behavior of the crack in the structure.

Some remarks can be made concerning the above hybrid displacement finite element procedure as follows:

(1) The fundamental question is that of convergence of the finite element procedure as the element size becomes smaller and smaller. In this regard, we first note that the singular nature (of $r^{-\frac{1}{2}}$ type) of stresses and strains is predominant in a small but finite region near the crack tip, as can be judged from the theory of elasticity solution. Thus, it can be seen that in a finite element solution of the crack problem, the singular stress terms must be included in a fixed region near the crack tip. The size of the so-called *singular* element should also be kept fixed at an *optimum* size*, even when the so-called *regular* elements are made smaller and smaller for convergence studies. It can be seen that if the size of the *singular* elements is also made progressively smaller and approaches zero the stress singularity effect will completely disappear and the solution will certainly not converge to the correct stress intensity factor. Since the far field solution outside a fixed region near the crack tip, can be approximated by polynomials, and since the assumed displacements are compatible, the convergence of

* One of the reviewers has brought to our attention that a similar discussion on the optimum size for singular elements is presented in *Crack Analysis by Hybrid Stress Method*, by C. H. Luk, Ph.D. Thesis, Department of Aeronautics, M.I.T. (1972).

the finite element solution in the far field can be established essentially following the arguments of Ref. [11]. In summary, to study convergence, we choose a fixed region near the crack tip where *singular* elements are used, and in the rest of the region regular elements are employed. These regular elements are made progressively smaller in size for convergence purposes. A detailed mathematical discussion of the convergence will be presented in a subsequent report.

(2) The present formulation leads essentially to a matrix displacement method. Since only four singular elements are used around the crack tip in the present study, one can develop the assembled stiffnes matrix of these four elements separately and combine it with the stiffness matrix of the rest of the structure, which can be developed through conventional compatible displacement finite element method. In a compatible displacement finite element method, for a quadrilateral element with 8 nodes along the boundary, the boundary displacements would be quadratic. Thus it is clear that the *regular* elements developed by conventional displacement method would be *compatible* with the *singular* elements of the present formulation.

3. Results for stress intensity factors

To illustrate the method discussed in this paper, several example problems have been solved and compared with other known theoretical solutions. These include: (a) a central

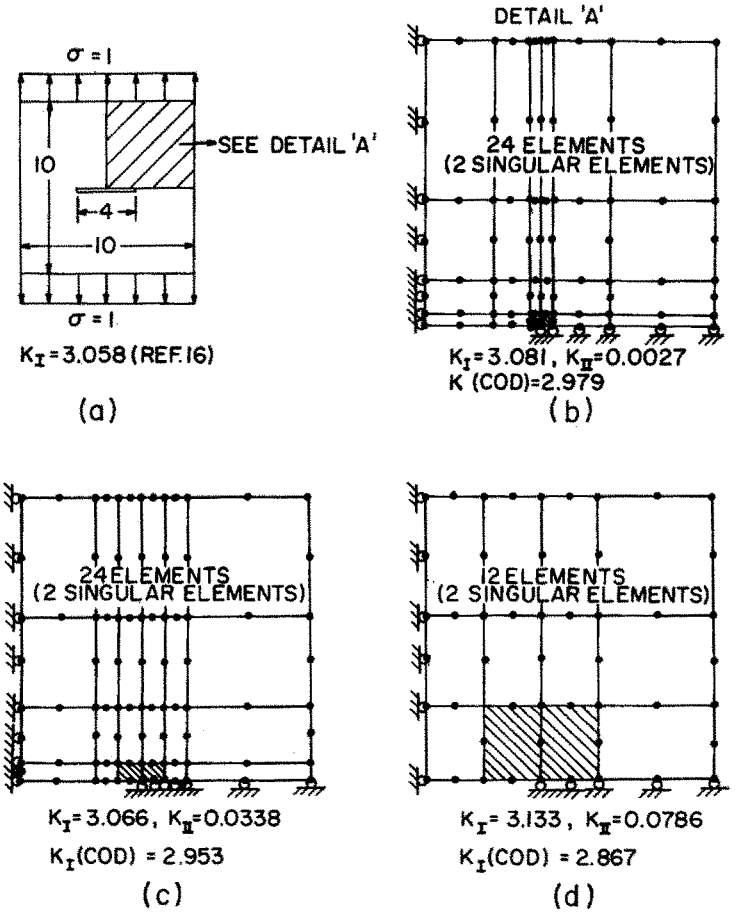

Figure 2. Element breakdown for a center cracked uniaxial tension plate.

crack in a finite, isotropic uniaxial tension plate; (b) a central crack in an orthotropic uniaxial tension plate; (c) a single-edge crack in an isotropic uniaxial tension plate; (d) an oblique edge crack in an isotropic uniaxial tension plate; (e) a central, quarter-circular crack in a finite, isotropic, biaxial tension plate; and (f) a central, quarter-circular crack in an isotropic uniaxial tension plate. Some of these problems have not hitherto been solved by finite element procedure. Close agreement in all cases, with the degrees of freedom of the entire structure ranging from 100 to 300, has been found between the present results and the theoretical results available in literature. A detailed discussion on these results has been presented in Ref. [25]. In this paper only the cases of: (1) a central crack in a tension plate; (2) an edge crack in a tension plate; and (3) a semi-circular crack in a tension plate loaded both uniaxially and biaxially are discussed.

The well studied problem of a central crack in a tension plate was re-analyzed to assess the accuracy and efficiency of the method used in this paper. Figure 2 shows a quadrant of the tension plate with three different nodal breakdowns. Also listed are the stress intensity factors directly computed by using Eqns. (25a, b) and the classical COD method*, for these three finite element models. In all cases, the hybrid displacement method yielded stress intensity factors which are much closer to the nominal value of $K_I = 3.058$ obtained from Ref. [16]. It is interesting to note that the stress intensity factor for the 24-element model with larger singular elements (Fig. 2c) was slightly closer to the nominal K_I than that with smaller singular elements (Fig. 2b). Stress intensity factor for the coarser element breakdown of Fig. 2d is 2.459% higher than the nominal value. The small residual K_{II} values in Fig. 2 are characteristic of the hybrid displacement method with embedded Mode I and Mode II singularities.

The same element breakdown as that shown in Fig. 2c was used to model a single-edge cracked (SEN) tension plate. Rollers located on the left side of the specimen shown in Fig. 2c were removed and the following stress intensity factors were obtained:

$$K_I = 5.260,\ K_{II} = -0.0674,\ K_I(\text{COD}) = 5.239\,.$$

The stress intensity factor obtained for a similar problem in Ref. [26] is 5.292, which is 0.602% larger than the K_I obtained by our analysis.

Figure 3 shows the element breakdown for half of a plate with a central, quarter-curved crack. The curved crack was approximated by straight line segments of the rectangular elements with the crack tip element oriented 45° to the axis of the plate. The same plate was used for biaxial and uniaxial loading. Table 1 shows the resultant K_I and K_{II} for biaxial and uniaxial tension loading. The slight difference in the computed and the reference stress intensity factors for the biaxially loaded tension plate is probably due to finite width effect in the computed stress intensity factor. Computed and reference stress intensity factors for the uniaxial tension plate, however, differed substantially for K_{II}.

The large discrepancies between the computed finite element solutions for K_I and K_{II} and those of [27] for uniaxial tension case involving quarter-circular crack led us to suspect the correctness of [27] results for uniaxial tension, in view of the good agreement between present results and the results of [27] for biaxial tension using identical plate geometry and element breakdown. A re-derivation of the bi-modal stress intensity factors for a segment-of-a-circle crack in an infinite plate subjected to uniaxial tension indeed revealed the discrepancy.

A re-derivation indicates that the correct forms of stress intensity factors for the same problem are:

* It should be mentioned that the COD used is the displacement solution obtained from the present finite element method.

TABLE 1

Stress intensity factor for a central, quarter-circle crack in a tension plate

	Computed		*Ref. [27] (Infinite plate)*		*Percent difference*	
	K_I	K_{II}	K_I	K_{II}	K_I	K_{II}
Biaxial tension	1.231	−0.524	1.201	−0.498	2.50%	5.37%
Uniaxial tension	0.812	−0.887	0.987	−0.482	−17.70%	84.32%

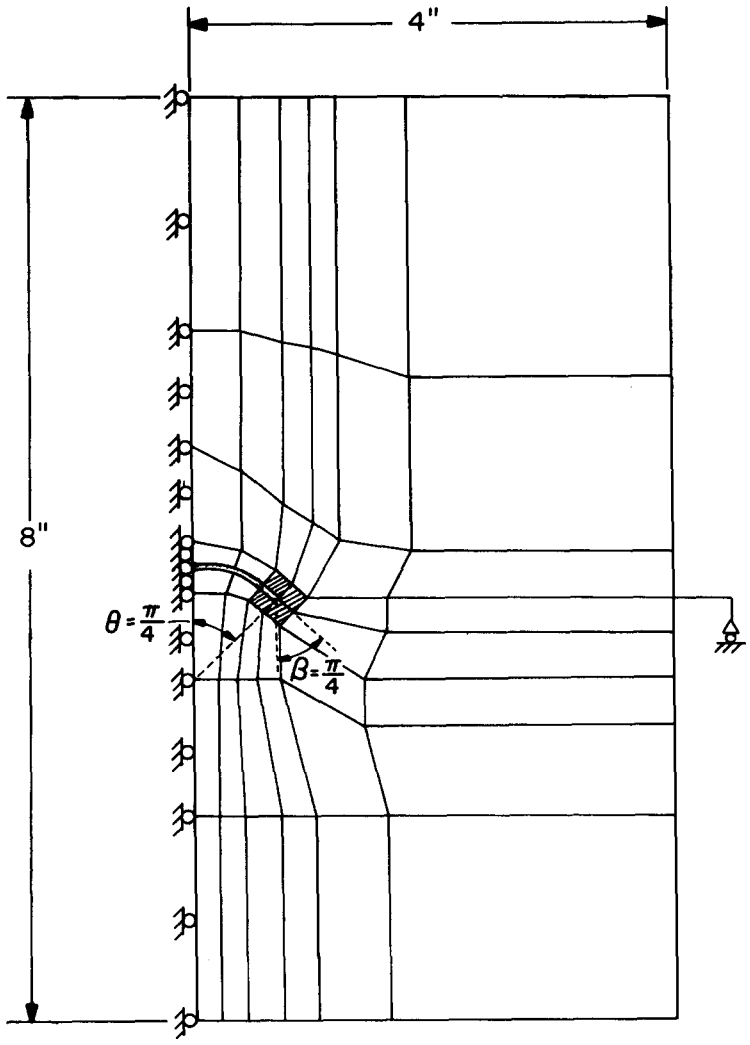

Figure 3. Element breakdown for a curved crack in a tension plate (biaxial and uniaxial tension).

$$K_{\mathrm{I}} = \frac{1}{2}\frac{(\pi \sin\theta)^{\frac{1}{2}}}{1+\sin^2(\theta/2)}\{\cos(\theta/2) - \cos[2\beta+(\theta/2)] - \cos(2\beta+\tfrac{3}{2}\theta)\sin^4(\theta/2) - 2\sin(2\beta+\tfrac{3}{2}\theta)\sin\theta\sin^2(\theta/2)\} \quad (26)$$

$$K_{\mathrm{II}} = \frac{1}{2}\frac{(\pi \sin\theta)^{\frac{1}{2}}}{1+\sin^2(\theta/2)}\{\sin(\theta/2) + \sin[2\beta+(\theta/2)] + \sin(2\beta+\tfrac{3}{2}\theta)\sin^4(\theta/2) + 2\sin(2\beta+\tfrac{3}{2}\theta)\cos\theta\sin^2(\theta/2)\}\,. \quad (27)$$

For the present problem of a quarter-circular crack, $\theta=\pi/4$ and $\beta=\pi/4$. The values of K_{I} and K_{II} as calculated from the re-derived forms given in Eqns. (26) and (27) are:

$$K_{\mathrm{I}} = 0.811 \text{ and } K_{\mathrm{II}} = -0.906$$

which agree well with the present finite element results (Table 1) of:

$$K_{\mathrm{I}} = 0.812 \text{ and } K_{\mathrm{II}} = -0.887\,.$$

A subsequent literature survey indicated that Hussain and Pu [28] also re-derived the stress intensity factors for a segment-of-circle crack in a uniaxial tension. It has been verified that the corrected forms for stress intensity as given in Eqns. (26) and (27) agree with the results of Hussain and Pu [28].

4. Conclusion

An assumed displacement hybrid finite element model which can efficiently solve problems in linear fracture mechanics has been developed. The developed model is also suitable for analyzing the elastic-plastic state in the vicinity of a crack tip. The utility of the new finite element procedure is demonstrated by the numerical results obtained for a central crack in a tension plate, a single-edge cracked tension plate, and a quarter-circular crack in a tension plate. These numerical results agreed well with known solutions.

Acknowledgement

This work was supported by the Air Force Office of Scientific Research under grant AFOSR-73-2478. The writers wish to express their appreciation for the encouragement given by Dr. W. J. Walker of AFOSR.

Appendices

A general quadrilateral element whose four corners have the physical, cartesian coordinates $(x_i, y_i, i=1, \ldots, 4)$ and whose boundary lines are general quadratic curves is transformed to a square element whose nondimensional coordinates ξ and η are such that $-1 \leqq \zeta \leqq 1$ and $-1 \leqq \eta \leqq 1$. Isoparametric transformations [29] are employed for this purpose. In the following we give the various assumed approximating functions, as discussed in the text, in terms of local element nondimensional coordinates ξ, η. The assumptions for the so-called *singular* element and a regular element are given separately.

Appendix 1. Assumed functions for a singular element

A1.1. *Element interior displacement field*:

$$\begin{Bmatrix} u_1 \\ u_2 \end{Bmatrix} = [U_{\mathrm{R}}]\{\beta\} + [U_{\mathrm{S}}]\begin{Bmatrix} K_{\mathrm{I}} \\ K_{\mathrm{II}} \end{Bmatrix} \quad (A.1)$$

where

$$[U_R] = \begin{bmatrix} 1,0,\xi,\eta,\xi^2,\eta^2,\xi\eta,\xi^2\eta,\xi\eta^2,0,0, & 0, & 0, & 0, & 0 \\ 0,1,0,\xi,0, & 0, & 0, & 0, & 0, \quad \eta,\xi^2,\eta^2, \quad \xi\eta,\xi^2\eta,\xi\eta^2 \end{bmatrix}$$

$$[\beta] = [\beta_1, \beta_2, \beta_3, \ldots, \beta_{15}]$$

and

$$[U_S] = 2\mu^{-1}(2r/\pi)^{\frac{1}{2}} \begin{bmatrix} \cos(\theta/2)\{(1-2\nu)+\sin^2(\theta/2)\}; & \sin(\theta/2)\{2(1-\nu)+\cos^2(\theta/2)\} \\ \sin(\theta/2)\{2(1-\nu)-\cos^2(\theta/2)\}; & -\cos(\theta/2)\{(1-2\nu)-\sin^2(\theta/2)\} \end{bmatrix}$$

Appendix 2. Independent element boundary displacement

$$\{v\}_s = [L_S]\{q\} \tag{A.2}$$

where for a singular element such as ADBE,

$$[v] = [v_{1AD}, v_{2AD}, v_{1DE}, v_{2DE}, v_{1EB}, v_{2EB}, v_{1BA}, v_{2BA}]$$
$$[q] = [q_1, q_2, \ldots, q_{16}] \quad \text{(see Fig. 1a)}.$$

The nonzero elements of matrix L_S, as assumed, are as follows (the subscript s is omitted in the equations below):

$$L_{1,1} = 1-r^{\frac{1}{2}}(\xi)\left(\frac{r_{11}-r_{01}}{r_{01}^{\frac{1}{2}}r_{11}-r_{01}r_{11}^{\frac{1}{2}}}\right) + \frac{r(\xi)}{(r_{01}r_{11})^{\frac{1}{2}}} \equiv L_{2,2}$$

$$L_{1,3} = \frac{r^{\frac{1}{2}}(\xi)r_{11}^{\frac{1}{2}}}{r_{01}^{\frac{1}{2}}r_{11}^{\frac{1}{2}}-r_{01}} - \frac{r(\xi)}{(r_{01}r_{11})^{\frac{1}{2}}-r_{01}} \equiv L_{2,4}$$

$$L_{1,5} = \frac{-r^{\frac{1}{2}}(\xi)r_{01}^{\frac{1}{2}}}{r_{11}-(r_{01}r_{11})^{\frac{1}{2}}} + \frac{r(\xi)}{r_{11}-(r_{01}r_{11})^{\frac{1}{2}}} \equiv L_{2,6}$$

$$L_{3,5} = -(\eta/2)+(\eta^2/2) \equiv L_{4,6}$$

$$L_{3,7} = 1-\eta^2 \equiv L_{4,8}$$

$$L_{3,9} = (\eta/2)+(\eta^2/2) \equiv L_{4,10}$$

$$L_{5,13} = -(\xi/2)+(\xi^2/2) \equiv L_{6,14}$$

$$L_{5,11} = 1-\xi^2 \equiv L_{6,12}$$

$$L_{5,8} = (\xi/2)+(\xi^2/2) \equiv L_{6,10}$$

$$L_{7,1} = 1-r^{\frac{1}{2}}(\eta)\left(\frac{r_{12}-r_{02}}{r_{02}^{\frac{1}{2}}r_{12}-r_{02}r_{12}^{\frac{1}{2}}}\right) + \frac{r(\eta)}{(r_{02}-r_{12})^{\frac{1}{2}}} \equiv L_{8,2}$$

$$L_{7,15} = \frac{r^{\frac{1}{2}}(\eta)r_{12}^{\frac{1}{2}}}{r_{02}^{\frac{1}{2}}r_{12}^{\frac{1}{2}}-r_{02}} - \frac{r(\eta)}{(r_{02}r_{12})^{\frac{1}{2}}-r_{02}} \equiv L_{8,16}$$

$$L_{7,13} = \frac{-r_0^{\frac{1}{2}}(\eta)r_{02}^{\frac{1}{2}}}{r_{12}-(r_{02}r_{12})^{\frac{1}{2}}} + \frac{r(\eta)}{r_{12}-(r_{02}r_{12})^{\frac{1}{2}}} \equiv L_{8,14}.$$

In the above, $r(\xi)$ is the actual value of the radial distance as measured from the crack tip to any point ξ $(-1 \leqq \xi \leqq 1)$ along the element boundary line AD (see Fig. 1). Similar definition holds for $r(\eta)$ along line AB. For clarity, it can be mentioned that the point $(\xi, \eta) \equiv (-1, -1)$ coincides with the crack tip for a singular element such as ABED, and thus $r(\xi = -1, \eta = -1) = 0$. Further definitions of quantities used above are:

$$r_{01} = r\,(\xi = 0, \eta = -1);\ r_{11} = r(\xi = 1, \eta = -1)$$
$$r_{02} = r\,(\eta = 0, \xi = -1);\ r_{12} = r(\eta = 1, \xi = -1)$$

Appendix 3. Assumed independent boundary tractions

The independently assumed tractions along the boundaries (which are in general curved) of an element, in terms of the nondimensional coordinates ξ, η are as follows.

$$\{T\}_s = [R]_s \{\alpha\} \tag{A.3}$$

where, for a singular element such as ADBE

$$[T]_s = [T_x^{AD}, T_y^{AD}, T_x^{DE}, T_y^{DE}, T_x^{BE}, T_y^{BE}, T_x^{AB}, T_y^{AB}]$$

The number of parameters α has been taken to be 13*. In order to insure a better approximation, these boundary tractions are generated from a boundary stress field which corresponds to an equilibrium solution. Thus, the boundary stresses are taken to be the respective values of the boundary of a stress field derived from a fictitious stress function in the interior of the element. That is, we assume a stress function,

$$\begin{aligned}\phi = {} & \alpha_1\xi^2 + \alpha_2\eta^2 + \alpha_3\xi\eta + \alpha_4\xi^3 + \alpha_5\eta^3 + \alpha_6\xi^2\eta \\ & + \alpha_7\xi\eta^2 + \alpha_8\xi^4 + \alpha_9\eta^4 + \alpha_{10}\xi^3\eta + \alpha_{11}\xi\eta^3\end{aligned} \tag{A.4}$$

and derive a self-equilibrating stress field,

$$\sigma_{xx} = \partial^2\phi/\partial y^2, \quad \sigma_{yy} = \partial^2\phi/\partial x^2 \quad \sigma_{xy} = -\partial^2\phi/\partial x\,\partial y \tag{A.5}$$

and evaluate their values at the boundary of the element. The boundary tractions are, then

$$T_i = \phi_{ij} v_j \tag{A.6}$$

where v_j are the direction cosines of a normal to the boundary. We notice that the 11 parameter boundary traction field as given by Eqns. (A.4) and (A.5) is free from any singularities. As has been discussed in the text, for a singular element, it is necessary to include a singular traction field. This is done there by properly calculating the boundary tractions, for a general element with curved boundaries, from a two-parameter singular stress field,

$$\sigma_{xx} = \frac{\alpha_{12}}{4(2\pi r)^{\frac{1}{2}}}\left(3\cos\frac{\theta}{2} + \cos\frac{5\theta}{2}\right) - \frac{\alpha_{13}}{4(2\pi r)^{\frac{1}{2}}}\left(7\sin\frac{\theta}{2} + \sin\frac{5\theta}{2}\right) \tag{A.7}$$

$$\sigma_{yy} = \frac{\alpha_{12}}{4(2\pi r)^{\frac{1}{2}}}\left(5\cos\frac{\theta}{2} - \cos\frac{5\theta}{2}\right) - \frac{\alpha_{13}}{4(2\pi r)^{\frac{1}{2}}}\left(\sin\frac{\theta}{2} - \sin\frac{5\theta}{2}\right) \tag{A.8}$$

$$\sigma_{xy} = -\frac{\alpha_{12}}{4(2\pi r)^{\frac{1}{2}}}\left(\sin\frac{\theta}{2} - \sin\frac{5\theta}{2}\right) + \frac{\alpha_{13}}{4(2\pi r)^{\frac{1}{2}}}\left(3\cos\frac{\theta}{2} + \cos\frac{5\theta}{2}\right). \tag{A.9}$$

From the values of these stresses at the boundary, the tractions are assumed once again, according to $T_i = \sigma_{ij} v_j$. The addition of the two traction fields as given in Eqns. (A.6), (A.7) and (A.8) give the 13 parameter traction field as indicated in Eqn. (A.3). It should be noted that since the above singular stress field also satisfies the equilibrium equations, and the

* This would insure that the matrix P_1 in Eqn. (20a) is square, and hence, if positive definite, can be inverted.

regular stress field as in Eqn. (A.5) is derived from a stress function, the boundary tractions as in Eqn. (A.3) which are assumed as a combination of the stress fields in Eqns. (A.5) and (A.6–8), correspond to an equilibrium field. This enhances the accuracy of the finite element method.

REFERENCES

[1] J. R. Rice, Mathematical Analysis in the Mechanics of Fracture, *Fracture*, Vol. II, (Edited by H. Liebowitz) Academic Press (1968) 192–308.

[2] A. S. Kobayashi, D. E. Maiden, B. J. Simon and S. Iida, *Application of the Method of Finite Element Analysis to Two-Dimensional Problems in Fracture Mechanics*, University of Washington, Department of Mechanical Engineering Report, October (1968).

[3] J. K. Chan, I. S. Tuba and W. K. Wilson, *Journal of Engineering Fracture Mechanics*, 2 (1970) 1–17.

[4] V. B. Watwood, The Finite Element Method for Prediction of Crack Behavior, *Nuclear Engineering and Design*, Vol. II (1969) 323–332.

[5] G. P. Anderson, V. L. Ruggles and G. S. Stikor, *International Journal of Fracture Mechanics*, 7, 1 (1971) 63–76.

[6] P. D. Hilton and G. C. Sih, Applications of the Finite Element Method to the Calculations of Stress Intensity Factors, *Methods of Analysis of Crack Problems* (Edited by G. C. Sih), Noordhoff International Publishing, Leyden (1973).

[7] P. Tong and T. H. H. Pian, *International Journal of Solids and Structures*, (1973) 313–321.

[8] E. Byskov, *International Journal of Fracture Mechanics*, 6, 2, (1970), 159–167.

[9] D. M. Tracey, *International Journal of Fracture Mechanics*, 3, 3 (1971) 255–266.

[10] P. Tong and T. H. H. Pian, *International Journal of Solids and Structures*, 3 865–879.

[11] N. J. Levy and P. V. Marcal, Three-Dimensional Elastic Plastic Stress Analysis for Fracture Mechanics, *Heavy Section Steel Technology Program, Fifth Annual Meeting*, Paper No. 11, Oak Ridge National Laboratories, March (1971).

[12] T. H. H. Pian, P. Tong and C. H. Luk, Elastic Crack Analysis by a Finite Element Hybrid Method, *Proceedings of the Third International Conference on Matrix Methods in Structural Mechanics*, Wright-Patterson Air Force Base, Ohio, November (1971).

[13] T. H. H. Pian, Element Stiffness Matrices for Boundary Compatibility and for Prescribed Boundary Stresses, *Proceedings of the First Conference of Matrix Methods in Structural Mechanics*, AFFDL-TR-66-80 (1967) 457–477.

[14] P. Tong, T. H. H. Pian and S. Lasry, A Hybrid-Element Approach to Crack Problems in Plane Elasticity, to appear in the *International Journal of Numerical Methods in Engineering*.

[15] O. L. Bowie, and D. M. Neal, *International Journal of Fracture Mechanics*, 6 (1970) 299–306.

[16] O. L. Bowie, and D. M. Neal, *Engineering Fracture Mechanics*, 2 (1970) 181–182.

[17] O. L. Bowie, C. E. Freese and D. M. Neal, *Solution of Plane Problems of Elasticity Utilizing Partitioning Concepts*, ASME paper 73-APM-C.

[18] J. A. H. Hult and F. A. McClintock, Elastic-Plastic Stress and Strain Distribution around Sharp Notches under Repeated Shear, *IXth International Congress of Applied Mechanics*, University of Brussels, 8 (1957) 51–58.

[19] M. F. Koskinen, *Journal of Basic Engineering*, Trans. ASME, 86, Series D (1963) 585–588.

[20] J. R. Rice and G. F. Rosengren, *Journal of Mechanics and Physics of Solids*, 16 (1968) 1–12.

[21] J. W. Hutchinson, *Journal of Mechanics and Physics of Solids*, 16 (1968) 13–31.

[22] J. W. Hutchinson, *Journal of Mechanics and Physics of Solids*, 16 (1968) 337–347.

[23] P. Tong, *International Journal of Numerical Methods in Engineering*, 2 (1960) 78–83.

[24] S. Atluri and T. H. H. Pian, *Journal of Structures and Mechanics*, 1 (1972) 1–43.

[25] S. Atluri, A. S. Kobayashi and M. Nakagaki, Application of an Assumed Displacement Hybrid Finite Element Procedure to Two-Dimensional Problems in Fracture Mechanics, submitted for presentation and publication at *The 15th Structures, Structural Dynamics and Materials Conference*, April 17–19, (1974) Las Vegas.

[26] B. Gross and J. E. Strawley, *Stress Intensity Factor for a Single-Edge-Notch Tension Specimen by Boundary Collocation of a Stress Function*, NASA TN D-2398, August (1964).

[27] G. C. Sih, P. C. Paris, and F. Erdogan, *Journal of Applied Mechanics*, Trans. of ASME, 29 (1962) 306–312.

[28] M. A. Hussain and S. L. Pu, *Journal of Applied Mechanics*, 38 (1971) 627–633.

[29] O. C. Zienkiewicz, *The Finite Element Method in Engineering Science*, McGraw-Hill, New York (1971).

RÉSUMÉ

Le mémoire a trait à une procédure pour le calcul des facteurs d'intensité des contraintes élastiques dans le cas de fissures de formes arbitraires soumises à état plan de tension ou de déformation. Un modèle de déplacements hypothétiques à éléments finis hybrides est utilisé, dans lequel les inconnues dans le système final d'équations algébriques sont les déplacements nodaux et les facteurs d'intensité des contraintes. Des éléments spéciaux, comportant leurs propres déplacements et champs de contraintes singuliers, sont utilisés dans une région déterminée voisine de l'extrémité de la fissure ; la compatibilité de déplacement entre les éléments est satisfaite en recourant à la technique de multiplication d'un Lagrangien. Des exemples numériques sont présentés, notamment : fissures centrales ou de bord dans des tôles soumises à tension, fissure en quart de cercle dans une tôle tendue. D'excellentes corrélations ont été établies avec les solutions disponibles pour chaque cas traité. On procède également à une discussion sur la convergence de la solution proposée.

ZUSAMMENFASSUNG

Dieser Bericht behandelt ein Verfahren zur Rechnung der elastischen Spannungsintensitätsfaktoren von Rissen beliebiger Form in ebenen Spannungs- und ebenen Verformungsproblemen. Man benützt ein festgelegtes Verschiebungsmodell hybrider endlicher Elementen indem die Unbekannten im Endgleichungssystem die Knotenverschiebungen und die elastischen Spannungsintensitätsfaktoren sind. Besondere Elemente, die eigene singuläre Verschiebungen und Spannungsfelder enthalten, werden in einem festgelegten Gebiet an der Rißspitze benützt, und die Komptabilität der Verschiebungen zwischen Elementen werden durch ein Multiplikationsverfahren von Lagrange erfüllt. Die angegebene Rechenbeispiele enthalten: Mittel- sowohl als Randrisse in Platten unter Zugspannung, und ein Viertelkreisriß in einer Platte unter Zugspannung. Ausgezeichnete Korrelation ergab sich mit allen zur Verfügung stehenden Lösungen in allen Fällen. Die Konvergenz der angegebenen Lösung wird auch besprochen.